



Original Article

Received: July 23, 2023
Revised: January 8, 2024
Accepted: January 11, 2024

Correspondence

Yong Eun Chung, MD, PhD
Department of Radiology,
Severance Hospital,
Yonsei University
College of Medicine,
50-1 Yonsei-ro, Seodaemun-gu,
Seoul 03722, Korea.
E-mail: yelv@yuhs.ac

Comparison of Volumetric Measurement Method With Region of Interest Drawing Method for Liver Fat Quantification

Hyunji Lee¹, Heejin Bae¹, Ja Kyung Yoon¹, June Park¹, and Yong Eun Chung^{1,2}

¹Department of Radiology, Severance Hospital, Yonsei University College of Medicine, Seoul, Korea
²Institute for Innovation in Digital Healthcare, Yonsei University, Seoul, Korea

Purpose: This study aimed to evaluate the feasibility of measuring liver fat using the volumetric measurement method (Fat_{vol}) by comparing it with the conventional 27-regions of interest drawing method (Fat_{roi}).

Materials and Methods: This retrospective study included 67 patients who underwent liver magnetic resonance imaging with fat quantification in August or September 2020. Two experienced abdominal radiologists measured the proton density fat fraction (PDFF) of the liver using the mDIXON-Quant sequence for each of two methods. The PDFF was measured twice with each method at intervals of at least 4 weeks to avoid recall bias. Measurement times were recorded. The intra-class correlation coefficient (ICC) was calculated for intra-exam repeatability, inter-reviewer reproducibility, and inter-exam agreement.

Results: Measurement times for Fat_{vol} were significantly shorter than for Fat_{roi} . Measurement times for Fat_{roi} and Fat_{vol} , respectively, for reviewer A were 209.4 ± 55.1 s and 137.2 ± 51.5 s in session 1, and 180.9 ± 37.3 s and 127.0 ± 46.1 s in session 2. For reviewer B, the times were 190.7 ± 30.1 s and 74.8 ± 27.4 s in session 1, and 174.6 ± 21.8 s and 64.1 ± 17.5 s in session 2. In all cases, $p < 0.001$. The mean PDFF values were $7.2\% \pm 6.4\%$ and $7.2\% \pm 6.5\%$ (sessions 1 and 2, respectively) for Fat_{roi} and $7.4\% \pm 6.0\%$ and $7.3\% \pm 6.1\%$ for Fat_{vol} for reviewer A. For reviewer B, they were $7.1\% \pm 6.6\%$ and $7.1\% \pm 6.6\%$ for Fat_{roi} and $7.4\% \pm 5.8\%$ and $7.4\% \pm 5.8\%$ for Fat_{vol} . The ICCs between measurement methods (0.998 and 0.995 for reviewers A and B, respectively), for Fat_{vol} within each reviewer (0.999 and 1.000 in sessions 1 and 2, respectively), and between reviewers (0.999) were excellent.

Conclusion: The measurement time could be significantly reduced using Fat_{vol} compared to Fat_{roi} while maintaining the consistency of the liver fat measurement values.

Keywords: Non-alcoholic fatty liver disease; Fat quantification; Magnetic resonance imaging; Proton density fat fraction; Fatty liver

This is an Open Access article distributed under the terms of the Creative Commons Attribution Non-Commercial License (<http://creativecommons.org/licenses/by-nc/4.0/>) which permits unrestricted non-commercial use, distribution, and reproduction in any medium, provided the original work is properly cited.

INTRODUCTION

Nonalcoholic fatty liver disease (NAFLD) occurs when fat accumulates in the liver without a specific cause. The disease presents with varying degrees of severity and includes

simple steatosis, nonalcoholic steatohepatitis (NASH), hepatic fibrosis, liver cirrhosis, and hepatocellular carcinoma (HCC) [1]. NAFLD is the most prevalent chronic liver disease in Western countries, affecting 30% of the general population [2]. In addition to morbidity and mortality, NAFLD is closely associated with the development of metabolic syndromes, including type 2 diabetes, obesity, dyslipidemia, and atherosclerotic cardiovascular disease [3–5]. For this reason, significant effort has been devoted to understanding the pathogenesis of NAFLD, and novel therapies based on these new findings are being tested in clinical trials [6].

Assessment of hepatic fat deposition is required for both the development of new therapies and follow-up of patients with NAFLD. Traditionally, a liver biopsy has been considered the reference standard for diagnosing liver fat deposition. However, performing a liver biopsy for fat analysis has limitations such as difficulty in repetition, sampling errors, and complications including bleeding [7–9]. As a result, there is an unmet need for non-invasive methods to evaluate hepatic steatosis, and imaging modalities have been implemented for this purpose. Ultrasound (US) and computed tomography (CT) have been used to evaluate hepatic steatosis. However, US is highly operator dependent, and the clinical implementation of US methods for hepatic steatosis assessment may be limited by a variety of vendor-specific techniques and cut-off values [10–12]. CT exposes patients to radiation and has limited sensitivity and specificity in diagnosing mild fatty liver disease [13–15]. In addition, various conditions such as superimposed iron, amiodarone, iodine contrast, glycogen overload, and hepatitis can act as confounding factors that increase liver attenuation [15]. Recently, the controlled attenuation parameter (CAP) has been used for the overall assessment of hepatic steatosis owing to its noninvasiveness and good diagnostic performance. Furthermore, with the development of the XL probe, hepatic steatosis can be accurately diagnosed even in obese patients. However, its use is still limited in patients with bowel interposition or masses in the right hepatic lobe. CAP values may also be affected by body mass index, the presence of diabetes mellitus or NAFLD/NASH, and even the probe used (M or XL) [16].

Hepatic steatosis can be accurately evaluated by magnetic resonance imaging (MRI). MRI-based fat quantification methods are robust and reliable because they are not affected by scanner characteristics, acquisition parameters, or field strength [17,18]. Furthermore, the method presents no concerns regarding radiation exposure and patient conditions such as ascites or obesity. The proton density fat fraction (PDFF) is defined as the ratio of unconfounded signals from the mobile protons of fat to unconfounded signals from the mobile protons of water [14,17]. The PDFF is optimal for screening, diagnosing, and monitoring hepatic steatosis and is already widely accepted as

a quantitative biomarker of hepatic steatosis [18,19]. Recently, owing to the complexity of both the acquisition and processing processes as well as limited spatial coverage, chemical shift-encoded MRI has been more widely performed than magnetic resonance spectroscopy [14]. However, there is currently no consensus regarding the best approach for deriving summary quantitative PDFF estimates from PDFF maps acquired across the whole liver [14]. Considering the heterogeneous nature of hepatic fat deposition, a method for measuring liver fat by drawing multiple large regions of interest (ROIs) was introduced [20–22]. Measurement using the 4-ROI (medial, lateral, anterior, and posterior) or 9-ROI paradigm (one in each of the Couinaud segments, including 4a and 4b) is generally recommended, but known limitations include the long time required for measurement, sensitivity to imaging artifacts, and inaccurate representation of PDFF if there is focal or regional fat deposition/sparing [23–25]. Recently, a commercially available program (Philips IntelliSpace Portal Client, Philips Healthcare, Best, The Netherlands) has provided volumetric measurement of PDFF through automated whole-liver segmentation. Although attempts have been made to take volumetric measurements of hepatic steatosis using in-house software or commercial software, previous studies have focused more on the accuracy of volumetric segmentation of the liver than on comparing the different methods available to measure fat by drawing ROIs, or did not demonstrate how much time could be reduced by using volumetric fat measurement compared to conventional methods [26–28]. In this study, in addition to comparing the liver fat measurement results, we measured the time required to perform fat quantification to confirm the efficacy of automated whole-liver segmentation. Hence, the purpose of this study was to investigate the feasibility of a volumetric liver fat measurement method (Fat_{vol}) compared with the conventional 27-regions of interest drawing method (Fat_{roi}).

MATERIALS AND METHODS

This retrospective study was approved by the Institutional Review Board of Severance Hospital (No.4-2021-0290), which waived the requirement for informed consent.

Patient Selection

This retrospective study included outpatients who underwent non-contrast liver MRI for NAFLD, alcoholic liver disease, chronic viral hepatitis, or autoimmune hepatitis in August or September 2020 ($n = 90$). The exclusion criteria were as follows: 1) patients who underwent liver surgery ($n = 5$), 2) patients who underwent loco-regional treatment such as trans-arterial chemoembolization or radiofrequency ablation

(n = 7), 3) patients with focal liver lesions larger than 1.5 cm in size (n = 10), and 4) patients who were diagnosed with infiltrative HCC (n = 1). Demographic patient characteristics, including age, sex, clinical diagnosis, surgical history, and treatment history were extracted from the electronic medical records of the patients. A total of 23 patients were excluded from the study. Finally, 67 patients were included in this study.

MRI Examination

All MRI scans were acquired using a 3.0-T MR scanner (Ingenia Elition X, Philips Healthcare, Best, The Netherlands) with a 32-channel phased-array torso coil. A 3D multi-echo GRE sequence (mDIXON-Quant) was used for liver fat quantification based on the survey scan, with the field of view set to include the whole liver. The magnetic resonance parameters were as follows: repetition time = 5.64 ms, echo time = 0.97 ms (shortest), delta echo time = 0.7 ms, echo train length = 6, slice thickness = 6 mm, flip angle = 3°, matrix 256 × 232 mm, field of view = 400 mm, numbers of excitations (NEX) = 1, sensitivity encoding (SENSE) factor = 2, and scan time = 15 s. After acquisition of the mDIXON-Quant sequence, water, fat, T2*, and R2* maps were automatically generated. In addition, axial T2-weighted spectral attenuated inversion recovery (SPAIR) fat-suppressed images, heavily T2-weighted images, pre-contrast T1-weighted images, and diffusion-weighted images were included in the magnetic resonance sequence.

MRI Post-Processing and Analysis

PDFF was measured independently by two radiologists (reviewer A, a senior radiological resident, and reviewer B, a radiologist with 4 years of experience in abdominal radiology) using two methods: Fat_{roi} and Fat_{vol}. For the Fat_{roi} method, the reviewers drew ROIs as large as possible in each of the Couinaud segments (including separate measurements for 4a and 4b) while avoiding major blood vessels, bile ducts, and artifacts on the fat map. Three ROIs were drawn per segment in different slices and a total of 27 values were acquired (Fig. 1). The measured values were recorded using a spreadsheet program, and the average PDFF was automatically calculated according to a pre-entered formula. Additionally, the total time from the start of drawing the first ROI to recording the final PDFF value was measured. For the Fat_{vol} method, PDFF was measured using commercially available software (Liver Health, IntelliSpace Portal Client, Philips Healthcare, Best, The Netherlands). First, the liver was automatically segmented, and the program presented axial, coronal, and sagittal views of the segmented area. Subsequently, the reviewers corrected the liver margin if unnecessary parts such as the gallbladder, major blood vessels, or other adjacent organs were included or if the liver parenchyma was not included. However, as exact segmentation

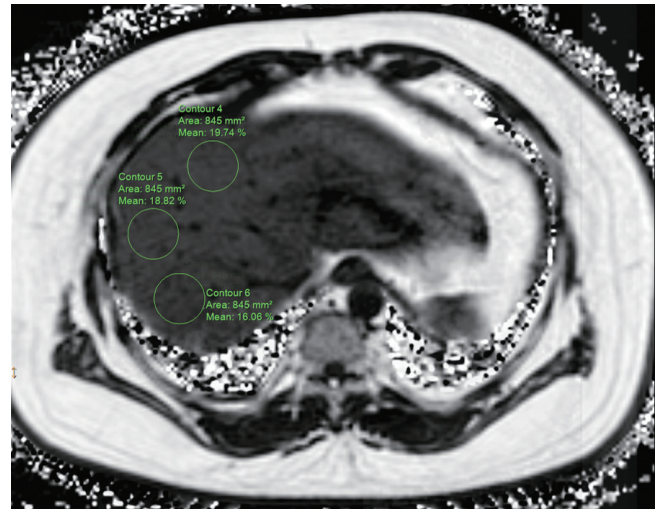


Fig. 1. Multiple Fat_{roi}. Three ROIs are drawn in each of nine segments of the liver for fat quantification. Fat_{roi}, 27-regions of interest drawing method; ROI, regions of interest.

along the liver boundary is time-consuming, the reviewers were asked to exclude structures other than the liver parenchyma (such as the gallbladder or heart) that have similar signal intensity to the liver, but to leave the boundary line drawn slightly inside the liver margin, as initially presented. This choice was made because the purpose of this study was not to accurately segment the liver but to evaluate the clinical feasibility of Fat_{vol}. Excluding a minimal volume of the liver parenchyma along the margin was not expected to significantly affect the final results (i.e., the volumetric PDFF value), whereas the inclusion of other structures was expected to have a large impact because fat is barely deposited in other organs. After confirming correct segmentation of the liver, the volumetric PDFF was calculated using a histogram of the calculated values. To remove noise (or error) and structures other than the liver within the volumetric ROI, the lower fat fraction margin was set to 0%, and the upper fat fraction margin was set based on the graph showing a normal distribution. After displaying the data in a histogram to obtain an appropriate value for liver fat quantification, the average value and standard deviation of liver fat were recorded (Fig. 2). The time from the start of the volumetric measurement to the recording of the PDFF value was also measured. Both reviewers were asked to measure the PDFF twice using each method to evaluate intra-observer variability. To prevent recall bias, measurements using the same method were performed with a time interval of 4–8 weeks.

Statistical Analysis

The intra-class correlation coefficient (ICC) was obtained for intra-exam repeatability, inter-reviewer reproducibility, and inter-exam agreement (Fig. 3). The one-way random method

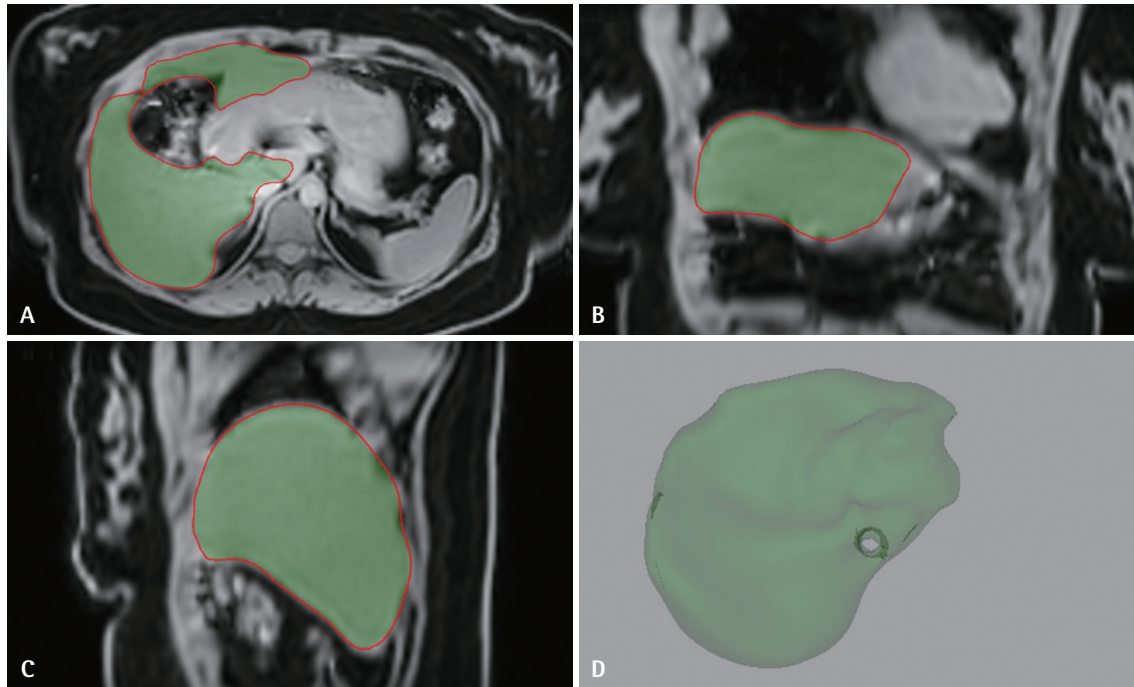


Fig. 2. Volumetric liver fat measurement method (Fat_{vol}). Automatic liver segmentation is conducted on axial (A), coronal (B) and sagittal (C) images, excluding organs such as the gallbladder, bowels, and stomach, for fat quantification. The result is presented as a 3D image (D).

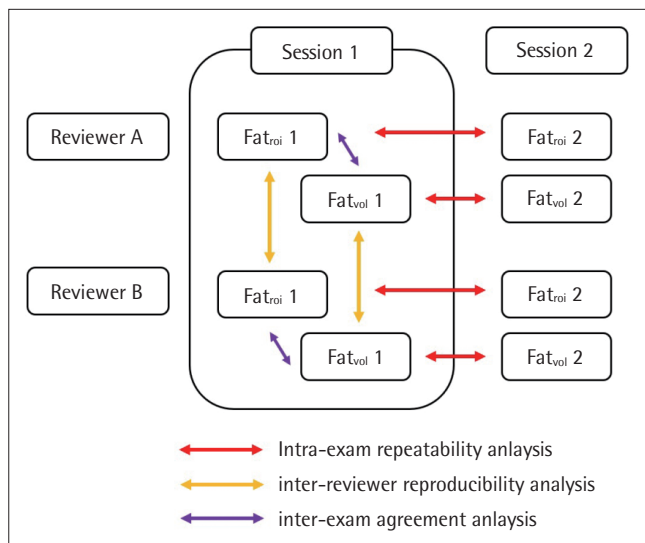


Fig. 3. Intra-exam repeatability (red arrows), inter-reviewer reproducibility (yellow arrows), and inter-exam agreement (purple arrows) analyses for conventional 27-ROI method (Fat_{ROI}). ROI, regions of interest; Fat_{ROI} , 27-regions of interest drawing method; Fat_{VOL} , volumetric liver fat measurement method.

was used for intra-exam repeatability. The two-way random method was used to assess inter-reviewer reproducibility. The two-way mixed method was used to determine inter-exam agreement. ICC values greater than 0.9 were considered to indicate excellent agreement. For ICC values between 0.75 and 0.90, the agreement was considered good, those between 0.50

and 0.75 were considered moderate, and those below 0.50, poor. The mean differences in measurement time within the reviewers and PDFFs were compared using a paired t-test. Bland-Altman analysis was used to assess intra-exam repeatability, inter-reviewer reproducibility, and inter-exam agreement. In addition, the correlation between Fat_{ROI} and Fat_{VOL} measured by both reviewers was evaluated using Pearson's correlation coefficient. The interpretation of the correlation coefficient was as follows: weak, 0–0.4; moderate, 0.4–0.7; and strong, 0.7–1. Statistical significance was set at $p < 0.05$. All statistical analyses were performed using SPSS version 25.0 (IBM Corp., Armonk, NY, USA).

RESULTS

Patient Demographics

Sixty-seven patients were included in this study (37 men and 30 women, age = 54.8 ± 13.3 years), and their demographics are summarized in Table 1.

Comparison of Measured PDFF and Measurement Time of the Two Methods

The average times for the Fat_{ROI} and Fat_{VOL} methods and the mean PDFF values measured using each method are listed in Table 2. The mean PDFF values were $7.2\% \pm 6.4\%$ and $7.2\% \pm 6.5\%$ (sessions 1 and 2, respectively) for Fat_{ROI} and $7.4\% \pm 6.0\%$

and $7.3\% \pm 6.1\%$ for Fat_{vol} for reviewer A. For reviewer B, they were $7.1\% \pm 6.6\%$ and $7.1\% \pm 6.6\%$ for Fat_{roi} and $7.4\% \pm 5.8\%$ and $7.4\% \pm 5.8\%$ for Fat_{vol} . Measurement times were significantly longer for Fat_{roi} than for Fat_{vol} for both reviewers and both measurement sessions (reviewer A, 209.4 ± 55.1 s to 137.2 ± 51.5 s in session 1, and 180.9 ± 37.3 s to 127.0 ± 46.1 s in session 2; reviewer B, 190.7 ± 30.1 s to 74.8 ± 27.4 s in session 1, and 174.6 ± 21.8 s to 64.1 ± 17.5 s in session 2). Measurement times significantly decreased in session 2 compared to session 1 for both reviewers and methods ($p < 0.001$) except for Fat_{vol} for reviewer B ($p = 0.060$).

Intra-Exam Repeatability Analyses

The ICCs for Fat_{roi} within each reviewer were excellent:

Table 1. Clinical characteristics of the study population (n = 67)

Characteristics	Value
Sex (male:female)	37 (55.2):30 (44.8)
Age (yr)	54.8 ± 13.3
Etiologies of liver disease	
HBV carrier	35 (52.2)
HCV carrier	4 (6.0)
Alcoholic liver disease	8 (11.9)
Non-alcoholic fatty liver disease	18 (26.9)
Autoimmune hepatitis	2 (3.0)

Values are presented as number (%) or mean \pm standard deviation. HBV, Hepatitis B carrier; HCV, Hepatitis C carrier.

Table 2. Measured PDFF, and the measurement time of both methods

Reviewer	Method	Session	PDFF (%)	p^\dagger	Measurement time (s)	p^*
A	Fat_{roi}	1	7.2 ± 6.4	0.631	209.4 ± 55.1	< 0.001
		2	7.2 ± 6.5		180.9 ± 37.3	
	Fat_{vol}	1	7.4 ± 6.0	0.135	137.2 ± 51.5	< 0.001
		2	7.3 ± 6.1		127.0 ± 46.1	
B	Fat_{roi}	1	7.1 ± 6.6	0.381	190.7 ± 30.1	< 0.001
		2	7.1 ± 6.6		174.6 ± 21.8	
	Fat_{vol}	1	7.4 ± 5.8	0.583	74.8 ± 27.4	0.060
		2	7.4 ± 5.8		64.1 ± 17.5	

Values are presented as mean \pm standard deviation.

*Comparison of measurement time; † Measured PDFF values between session 1 and session 2 when each reviewer measured using the same methods. PDFF, proton density fat fraction; Fat_{roi} , 27-regions of interest drawing method; Fat_{vol} , volumetric liver fat measurement method.

Table 3. Intra-exam repeatability analyses of Fat_{roi} and Fat_{vol}

Reviewer	Comparison*	ICC	95% CI	Mean difference (%)	95% LOA (lower to upper)
A	Fat_{roi} 1 vs. Fat_{roi} 2	0.997	0.995–0.998	0.029	-0.963 to 1.021
	Fat_{vol} 1 vs. Fat_{vol} 2	0.999	0.999–1.000	0.054	-0.520 to 0.628
B	Fat_{roi} 1 vs. Fat_{roi} 2	0.999	0.998–0.999	0.037	-0.623 to 0.696
	Fat_{vol} 1 vs. Fat_{vol} 2	1.000	1.000–1.000	0.006	-0.168 to 0.180

Lower LOA: mean difference -1.96 SD, upper LOA: mean difference +1.96 SD.

*Numbers represent each session 1 and session 2.

ICC, intra-class correlation coefficient; CI, confidence interval; LOA, limits of agreement; Fat_{roi} , 27-regions of interest drawing method; Fat_{vol} , volumetric liver fat measurement method; SD, standard deviation.

0.997, 95% confidence interval (CI) 0.995–0.998 for reviewer A and 0.999, 95% CI 0.998–0.999 for reviewer B. The ICCs for Fat_{vol} within each reviewer were also excellent (0.999, 95% CI 0.999–1.000 for reviewer A and 1.000, 95% CI 1.000–1.000 for reviewer B) (Table 3). The 95% limits of agreement (LOA) ranged from -0.963% to 1.021% when using Fat_{roi} and from -0.520% to 0.628% when using Fat_{vol} for reviewer A. For Reviewer B, the 95% LOA ranged from -0.623% to 0.696% when using Fat_{roi} and from -0.168% to 0.180% when using Fat_{vol} (Table 3 and Fig. 4).

Inter-Reviewer Reproducibility between the Fat_{roi} and Fat_{vol} Methods

The ICCs between reviewers were excellent for both Fat_{roi} (0.994, 95% CI 0.991–0.997) and Fat_{vol} (0.999, 95% CI 0.998–0.999) (Table 4). The 95% LOA ranged from -0.906% to 1.086% when using Fat_{roi} and from -0.466% to 0.561% when using Fat_{vol} (Table 4 and Fig. 5).

Inter-Exam Agreement between the Fat_{roi} and Fat_{vol} Methods

The ICCs between the two methods (0.998, 95% CI 0.996–0.999 for reviewer A and 0.995, 95% CI 0.991–0.997 for reviewer B) were excellent (Table 5). This suggests that the two methods have excellent inter-exam reproducibility. The 95% LOA ranged from -1.092% to 1.470% for reviewer A and from -1.383% to 2.036% for reviewer B (Table 5 and Fig. 6).

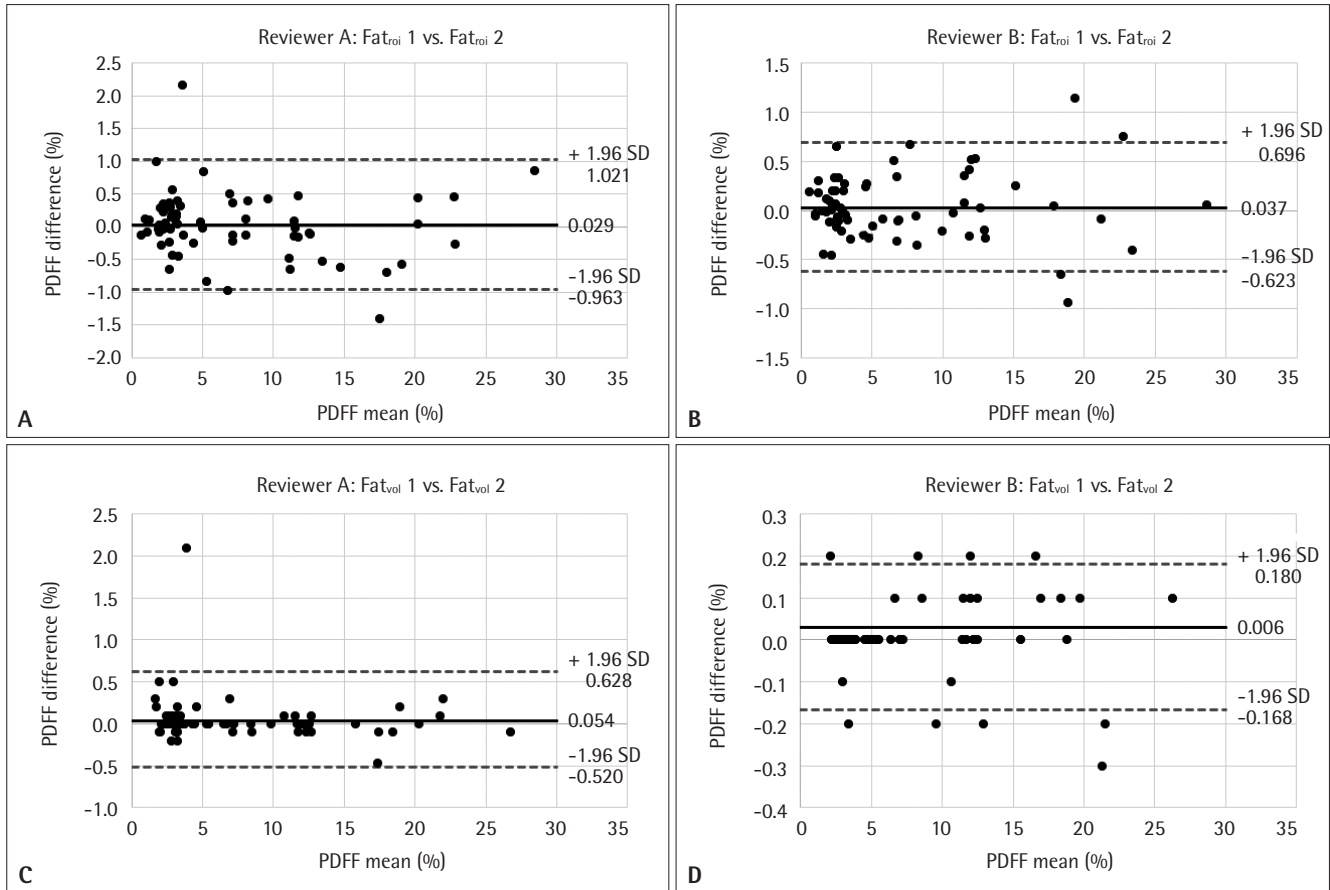


Fig. 4. Bland–Altman plots of intra-exam repeatability for Fat_{roi} for reviewer A (A) and reviewer B (B), and for Fat_{vol} for reviewer A (C) and (D) reviewer B. The dotted lines showed LOA and the solid line showed the mean of the differences. Fat_{roi} , 27–regions of interest drawing method; Fat_{vol} , volumetric liver fat measurement method; PDFF, proton density fat fraction; SD, standard deviation; LOA, limits of agreement.

Table 4. Inter-reviewer reproducibility of Fat_{roi} and Fat_{vol}

Method	Comparison	ICC	95% CI	Mean difference (%)	95% LOA (lower to upper)
Fat_{roi}	Reviewer A vs. B	0.994	0.991–0.997	0.090	-0.906 to 1.086
Fat_{vol}	Reviewer A vs. B	0.999	0.998–0.999	0.048	-0.466 to 0.561

Lower LOA: mean difference -1.96 SD, upper LOA: mean difference +1.96 SD.

Fat_{roi} , 27–regions of interest drawing method; Fat_{vol} , volumetric liver fat measurement method; ICC, intra-class correlation coefficient; CI, confidence interval; LOA, limits of agreement; SD, standard deviation.

The Pearson's correlation coefficient between Fat_{vol} and Fat_{roi} was 0.996 for reviewer A ($p < 0.001$) and 0.997 for reviewer B ($p < 0.001$), indicating a strong correlation between the two methods for both reviewers (Supplementary Fig. 1).

DISCUSSION

The results of this study demonstrate that use of the Fat_{vol} method could reduce liver fat measurement times significantly compared to the conventional Fat_{roi} method while preserving inter- and intra-exam reproducibility. The measured PDFF values were similar for the two methods. Furthermore, measure-

ment times further decreased in session 2 compared to session 1, suggesting that as researchers became familiar with the methods, they measured more quickly. Thus, measurement time could be further reduced with experience.

According to previous studies, the reproducibility and repeatability of liver fat measurements improve as the liver sampling area increases in size with a higher number of ROIs [22]. This might be due to the spatial heterogeneity of liver fat deposition because the segmental variation of fat deposition in the liver has been reported as approximately 12.5%–14.2% [29]. Furthermore, in previous studies, fat deposition was higher in the right lobe of the liver than in the left lobe, with or without a significant difference, whereas variability in fat

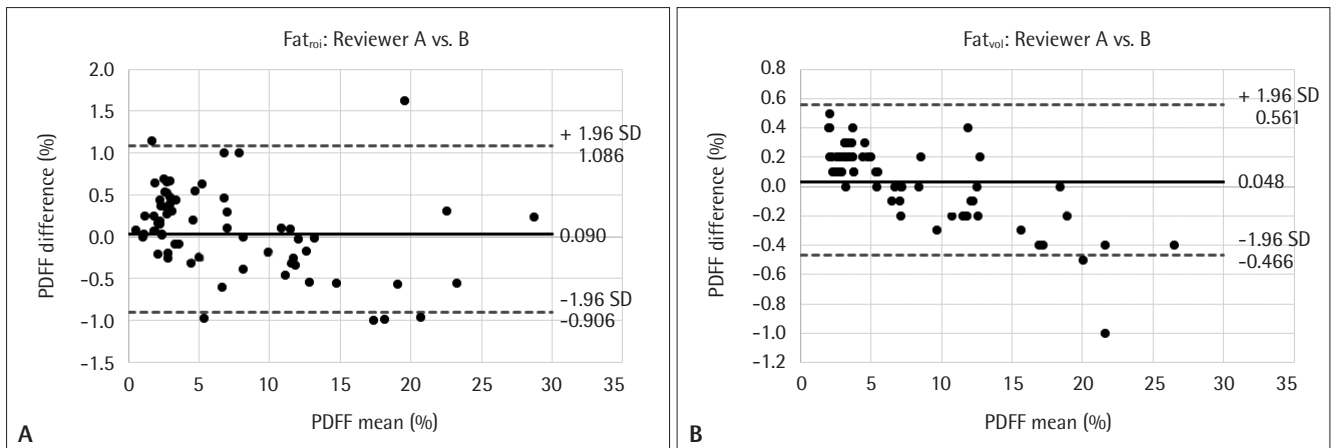


Fig. 5. Bland-Altman plots of inter-reviewer reproducibility of Fat_{roi} (A) and Fat_{vol} (B). The dotted lines showed LOA and the solid line showed the mean of the differences. Fat_{roi} , 27-regions of interest drawing method; Fat_{vol} , volumetric liver fat measurement method; PDFF, proton density fat fraction; SD, standard deviation; LOA, limits of agreement.

Table 5. Inter-exam reproducibility between Fat_{roi} and Fat_{vol}

Reviewer	Comparison	ICC	95% CI	Mean difference (%)	95% LOA (lower to upper)
A	Fat_{roi} vs. Fat_{vol}	0.998	0.996–0.999	0.189	-1.902 to 1.470
B	Fat_{roi} vs. Fat_{vol}	0.995	0.991–0.997	0.327	-1.383 to 2.036

Lower LOA: mean difference -1.96 SD, upper LOA: mean difference +1.96 SD.

ICC, intra-class correlation coefficient; CI, confidence interval; LOA, limits of agreement; Fat_{roi} , 27-regions of interest drawing method; Fat_{vol} , volumetric liver fat measurement method; LOA, limits of agreement; SD, standard deviation.

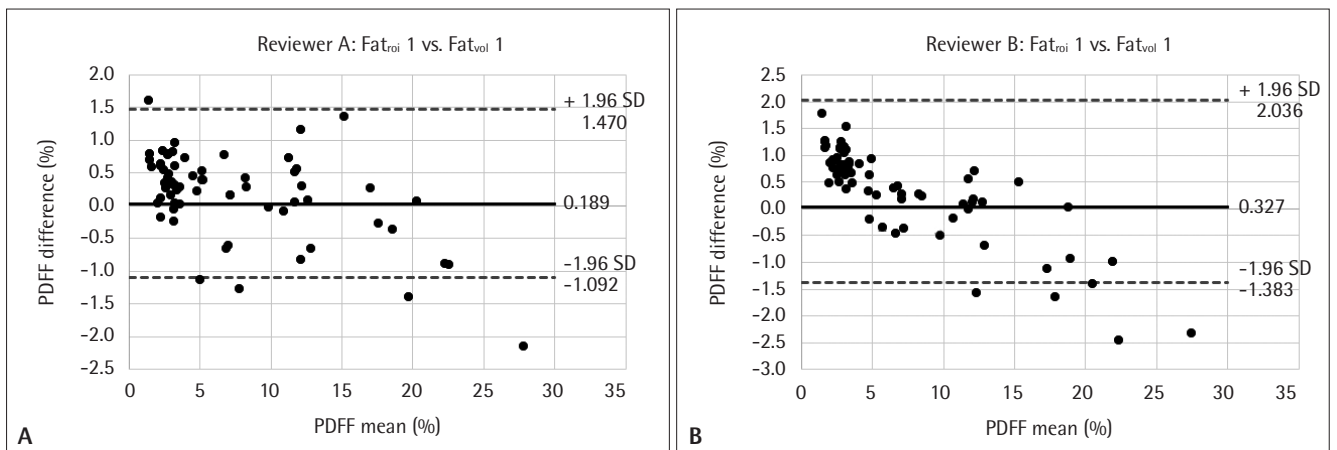


Fig. 6. Bland-Altman plots of inter-exam agreement of Fat_{roi} and Fat_{vol} for reviewer A (A) and reviewer B (B). The dotted lines showed LOA and the solid line showed the mean of the differences. Fat_{roi} , 27-regions of interest drawing method; Fat_{vol} , volumetric liver fat measurement method; PDFF, proton density fat fraction; SD, standard deviation; LOA, limits of agreement.

deposition was higher in the left lobe than in the right lobe [29,30]. However, a higher number of ROIs increases the time and labor intensity burden; hence, 4-ROI measurements have been suggested as a reasonable compromise between time burden and accuracy [21,22,30]. These simplified methods could be used in daily practice but might not be appropriate for clinical trials of new therapeutic drugs or treatment methods. Ideally, a method that samples from all of the imaged liver parenchyma should be used [31]. Whole-liver fat measurement has been

attempted in previous studies [26,27,29,31]; however, it has not been readily applied in clinical practice because of the lack of easily available software. A previous study showed a good correlation between Fat_{vol} and Fat_{roi} measured using a commercialized program, regardless of NAFLD severity [28]. These results are comparable with those of our study. In addition to agreement with these previous results, our study showed good agreement of Fat_{vol} values measured by two reviewers and demonstrated that using the Fat_{vol} method took

significantly less time than the Fat_{roi} method. Furthermore, the range of the LOA was smaller for Fat_{vol} than for Fat_{roi} within each reviewer and between the two reviewers, suggesting that Fat_{vol} might be less affected by the heterogeneity of fat deposition in the liver than Fat_{roi} .

In a study by Campo et al. [22], measurement times decreased from 113–150 s to 69–82 s (approximately 28%–51% reduction) with a reduction in the number of ROIs from 12 to 4. The absolute measurement time was longer in our study than in their study, possibly because of differences in the definition of the start and end times. However, using Fat_{vol} rather than Fat_{roi} could achieve similar reduction (30%–63%) in the measurement time without sacrificing the measurement area.

Measurement times decreased in session 2 compared to session 1 for both reviewers and both methods (Fat_{roi} , 8%–14% reduction; Fat_{vol} , 7%–14% reduction). Furthermore, the measurement time was shorter for the more experienced reviewer (reviewer B) than for the less experienced reviewer (reviewer A). These results suggest that measurement times can be reduced with increasing experience. Considering that only two measurement sessions were performed in this study, we expect even more reduction as radiologists gain experience, and hope to confirm this in a future study.

This study had some limitations. First, most of the included patients had diffuse liver disease. However, because PDFF is usually evaluated in patients with suspected fat deposition, our results may be suitable for actual clinical situations. Second, only Fat_{roi} with 27 ROIs was compared with Fat_{vol} . Third, pathology was not used as a reference standard. As the accuracy of PDFF measured on MRI scans has already been established, this study focused on the inter- and intra-reproducibility and repeatability between methods and reviewers, as well as measurement time. Lastly, in patients with severe fatty liver disease, the heterogeneity of fat deposition in the liver increases, but this study did not include patients with severe fatty liver disease.

In conclusion, the measurement time of PDFF could be reduced by 30%–63% using Fat_{vol} compared to Fat_{roi} , while maintaining the consistency of the measured values. Therefore, compared to the conventional Fat_{roi} method, the Fat_{vol} method is expected to improve the workflow while maintaining measurement accuracy.

Supplementary Materials

The online-only Data Supplement is available with this article at <https://doi.org/10.13104/imri.2023.0020>.

Availability of Data and Material

The datasets generated or analyzed during the study are available from the corresponding author on reasonable request.

Conflicts of Interest

Yong Eun Chung who is on the editorial board of the *Investigative Magnetic Resonance Imaging* was not involved in the editorial evaluation or decision to publish this article. All remaining authors have no competing interests to declare that are relevant to the content of this article.

Author Contributions

Conceptualization: Yong Eun Chung. Data curation: Hyunji Lee, Heejin Bae. Formal analysis: Hyunji Lee. Investigation: Hyunji Lee, Heejin Bae. Methodology: Heejin Bae. Project administration: Yong Eun Chung. Resources: Hyunji Lee, Heejin Bae. Software: Hyunji Lee, Heejin Bae. Supervision: Yong Eun Chung. Validation: Ja Kyung Yoon, June Park. Visualization: Hyunji Lee. Writing—original draft: Hyunji Lee. Writing—review & editing: Ja Kyung Yoon, June Park, Yong Eun Chung.

ORCID iDs

Hyunji Lee	https://orcid.org/0000-0001-7072-0001
Heejin Bae	https://orcid.org/0000-0002-1227-8646
Ja Kyung Yoon	https://orcid.org/0000-0002-3783-977X
June Park	https://orcid.org/0000-0003-1131-9730
Yong Eun Chung	https://orcid.org/0000-0003-0811-9578

Funding Statement

This work was supported by the National Research Foundation of Korea (NRF) grant funded by the Korean government (MIST) (2022 R1A2C101141111).

Acknowledgments

None

REFERENCES

- Perumpail BJ, Khan MA, Yoo ER, Cholankeril G, Kim D, Ahmed A. Clinical epidemiology and disease burden of nonalcoholic fatty liver disease. *World J Gastroenterol* 2017;23:8263–8276.
- Angulo P. Obesity and nonalcoholic fatty liver disease. *Nutr Rev* 2007;65(6 Pt 2):S57–S63.
- Angulo P. Nonalcoholic fatty liver disease. *N Engl J Med* 2002;346:1221–1231.
- Adams LA, Waters OR, Knuiman MW, Elliott RR, Olynyk JK. NAFLD as a risk factor for the development of diabetes and the metabolic syndrome: an eleven-year follow-up study. *Am J Gastroenterol* 2009;104:861–867.
- Schwenzer NF, Springer F, Schraml C, Stefan N, Machann J, Schick F. Non-invasive assessment and quantification of liver steatosis by ultrasound, computed tomography and magnetic resonance. *J Hepatol* 2009;51:433–445.
- Reimer KC, Wree A, Roderburg C, Tacke F. New drugs for NAFLD: lessons from basic models to the clinic. *Hepatol Int* 2020;14:8–23.
- Ratziu V, Charlotte F, Heurtier A, et al. Sampling variability of

- liver biopsy in nonalcoholic fatty liver disease. *Gastroenterology* 2005;128:1898-1906.
8. Rockey DC, Caldwell SH, Goodman ZD, Nelson RC, Smith AD. Liver biopsy. *Hepatology* 2009;49:1017-1044.
 9. Boyd A, Cain O, Chauhan A, Webb GJ. Medical liver biopsy: background, indications, procedure and histopathology. *Frontline Gastroenterol* 2020;11:40-47.
 10. Machado MV, Cortez-Pinto H. Non-invasive diagnosis of non-alcoholic fatty liver disease. A critical appraisal. *J Hepatol* 2013;58:1007-1019.
 11. Han A, Zhang YN, Boehringer AS, et al. Assessment of hepatic steatosis in nonalcoholic fatty liver disease by using quantitative US. *Radiology* 2020;295:106-113.
 12. Ferraioli G, Kumar V, Ozturk A, Nam K, de Korte CL, Barr RG. US attenuation for liver fat quantification: an ALUM-RSNA QIBA pulse-echo quantitative ultrasound initiative. *Radiology* 2022;302:495-506.
 13. Fazel R, Krumholz HM, Wang Y, et al. Exposure to low-dose ionizing radiation from medical imaging procedures. *N Engl J Med* 2009;361:849-857.
 14. Starekova J, Reeder SB. Liver fat quantification: where do we stand? *Abdom Radiol (NY)* 2020;45:3386-3399.
 15. Starekova J, Hernando D, Pickhardt PJ, Reeder SB. Quantification of liver fat content with CT and MRI: state of the art. *Radiology* 2021;301:250-262.
 16. Sirlin R, Sporea I. Controlled attenuation parameter for quantification of steatosis: which cut-offs to use? *Can J Gastroenterol Hepatol* 2021;2021:6662760.
 17. Reeder SB, Hu HH, Sirlin CB. Proton density fat-fraction: a standardized MR-based biomarker of tissue fat concentration. *J Magn Reson Imaging* 2012;36:1011-1014.
 18. Yokoo T, Serai SD, Pirasteh A, et al. Linearity, bias, and precision of hepatic proton density fat fraction measurements by using MR imaging: a meta-analysis. *Radiology* 2018;286:486-498.
 19. Reeder SB, Cruite I, Hamilton G, Sirlin CB. Quantitative assessment of liver fat with magnetic resonance imaging and spectroscopy. *J Magn Reson Imaging* 2011;34:729-749.
 20. Larson SP, Bowers SP, Palekar NA, Ward JA, Pulcini JP, Harrison SA. Histopathologic variability between the right and left lobes of the liver in morbidly obese patients undergoing Roux-en-Y bypass. *Clin Gastroenterol Hepatol* 2007;5:1329-1332.
 21. Bonekamp S, Tang A, Mashhood A, et al. Spatial distribution of MRI-determined hepatic proton density fat fraction in adults with nonalcoholic fatty liver disease. *J Magn Reson Imaging* 2014;39:1525-1532.
 22. Campo CA, Hernando D, Schubert T, Bookwalter CA, Pay AJV, Reeder SB. Standardized approach for ROI-based measurements of proton density fat fraction and R2* in the liver. *AJR Am J Roentgenol* 2017;209:592-603.
 23. Tang A, Tan J, Sun M, et al. Nonalcoholic fatty liver disease: MR imaging of liver proton density fat fraction to assess hepatic steatosis. *Radiology* 2013;267:422-431.
 24. Hines CD, Frydrychowicz A, Hamilton G, et al. T₁ independent, T₂* corrected chemical shift based fat-water separation with multi-peak fat spectral modeling is an accurate and precise measure of hepatic steatosis. *J Magn Reson Imaging* 2011;33:873-881.
 25. Bastati N, Feier D, Wibmer A, et al. Noninvasive differentiation of simple steatosis and steatohepatitis by using gadoxetic acid-enhanced MR imaging in patients with nonalcoholic fatty liver disease: a proof-of-concept study. *Radiology* 2014;271:739-747.
 26. Stocker D, Bashir MR, Kannengiesser SAR, Reiner CS. Accuracy of automated liver contouring, fat fraction, and R2* measurement on gradient multiecho magnetic resonance images. *J Comput Assist Tomogr* 2018;42:697-706.
 27. Wang K, Mamidipalli A, Retson T, et al. Automated CT and MRI liver segmentation and biometry using a generalized convolutional neural network. *Radiol Artif Intell* 2019;1:180022.
 28. Zhang QH, Zhao Y, Tian SF, et al. Hepatic fat quantification of magnetic resonance imaging whole-liver segmentation for assessing the severity of nonalcoholic fatty liver disease: comparison with a region of interest sampling method. *Quant Imaging Med Surg* 2021;11:2933-2942.
 29. Vu KN, Gilbert G, Chalut M, Chagnon M, Chartrand G, Tang A. MRI-determined liver proton density fat fraction, with MRS validation: comparison of regions of interest sampling methods in patients with type 2 diabetes. *J Magn Reson Imaging* 2016;43:1090-1099.
 30. Hong CW, Wolfson T, Sy EZ, et al. Optimization of region-of-interest sampling strategies for hepatic MRI proton density fat fraction quantification. *J Magn Reson Imaging* 2018;47:988-994.
 31. Procter AJ, Sun JY, Malcolm PN, Toms AP. Measuring liver fat fraction with complex-based chemical shift MRI: the effect of simplified sampling protocols on accuracy. *BMC Med Imaging* 2019;19:14.